DIFFUSE

An implicit/explicit/time-independent second-order diffusion solver

Peter Woitke

November 2017

Definitions

symbol	description	unit
z	vertical coordinate	cm
$n_{\langle \mathrm{H} \rangle}$	hydrogen nuclei density	cm^{-3}
$\rho = \mu_\mathrm{H}\, n_{\langle \mathrm{H} \rangle}$	gas mass density	$\mathrm{g\,cm}^{-3}$
$\mu_\mathrm{H} = \sum_k m_k \epsilon_k$	proportionality constant	g
m_k	mass of element k	g
ϵ_k	abundance of element k with respect to hydrogen	-
D	diffusion coefficient	$\mathrm{cm}^2\,\mathrm{s}^{-1}$

1 The diffusion problem

The motion of elements in a planetary atmosphere will be considered to be diffusive. There are two effects to consider: (a) gains and losses through the boundaries and (b) local source and sink terms due to the formation, drift, and evaporation of solids or liquids particles (precipitation).

Examples for processes of type (a) are the outgasing of elements from the rock forming the surface of the planet (the lower boundary of the atmosphere), and the loss of certain elements at the top of the atmosphere (Jeans escape).

The diffusive flux $\vec{j}_k$ [$\mathrm{cm}^{-2}\mathrm{s}^{-1}$] of an element k is given by its concentration gradient, which is known as Fick's first law (see e.g. Bringuier, 2013)

$$\vec{j}_k = -n_{\langle \mathrm{H} \rangle} D\, \nabla \epsilon_k \tag{1}$$

and the local gains and losses [$\mathrm{cm}^{-3}\mathrm{s}^{-1}$] on the right hand side of the continuity equation for element k is given by the divergence of the diffusive flux (Fick's second law) as

$$\frac{\partial (n_{\langle \mathrm{H} \rangle}\, \epsilon_k)}{\partial t} + \nabla (\vec{v}\, n_{\langle \mathrm{H} \rangle} \epsilon_k) \;=\; -\nabla \vec{j}_k + S_k \;, \tag{2}$$

where S_k are additional local source/sink terms [$\mathrm{cm}^{-3}\,\mathrm{s}^{-1}$], for example when dust grains grow or evaporate in the atmosphere. Combining these two equations we find the diffusion-reaction equation

$$\frac{\partial (n_{\langle \mathrm{H} \rangle}\, \epsilon_k)}{\partial t} + \nabla (\vec{v}\, n_{\langle \mathrm{H} \rangle} \epsilon_k) \;=\; \nabla \left(n_{\langle \mathrm{H} \rangle} D\, \nabla \epsilon_k \right) + S_k \;. \tag{3}$$

1.1 Static planeparallel atmosphere

We assume that the gas in the atmosphere is quasi-static $\vec{v} = 0$, and we assume the atmosphere to have plane-parallel geometry $\nabla \rightarrow \frac{d}{dz}$, in which case we find

$$\boxed{\frac{d(n_{\langle \mathrm{H} \rangle}\, \epsilon_k)}{dt} \;=\; \frac{d}{dz}\left(n_{\langle \mathrm{H} \rangle} D\, \frac{d\epsilon_k}{dz} \right) + S_k} \tag{4}$$

1.2 The diffusion constant

The gas-kinetic diffusion constant is given by

$$D_{\rm micro} \;=\; \frac{1}{3}\, v_{\rm th}\, \ell \;, \tag{5}$$

where $\ell = 1/(\sigma\, n)$ is the mean free path, n the total gas particle density and $\sigma \approx 2.1 \times 10^{-15}\,{\rm cm}^2$ a typical cross-section for a H_2-rich gas where the thermal velocity is defined as $v_{\rm th} = \sqrt{8kT/(\pi\mu)}$ (Woitke & Helling, 2003). This microphysical diffusion constant is often negligible in planetary atmospheres.

Instead, mixing by turbulent motions is usually the dominant mixing process. We describe this mixing by an effective diffusion coefficient which normally is much larger than $D_{\rm micro}$. The turbulent diffusion coefficient is roughly given by

$$D_{\rm mix} \;\approx\; \langle v_z \rangle\, H_p \;, \tag{6}$$

where $\langle v_z \rangle$ is the root-mean-square average of vertical velocities in the atmosphere, at height z. In the convective layer, $\langle v_z \rangle \approx v_{\rm conv}$ is the convective velocity which is a part of the stellar atmosphere model and results from the application of mixing length theory. Above the convective layer, where the Schwarzschild criterion for convection is false, $\langle v_z \rangle$ will decrease rapidly with increasing z, but will not be entirely zero due to convective overshoot. We apply a powerlaw in $\log p$ to approximate this behaviour

$$\log\langle v_z \rangle \;=\; \log v_{\rm conv} - \beta \cdot \max\{0, \log p_{\rm conv} - \log p(z)\} \tag{7}$$

with free parameter $\beta \approx 0.5 \,...\, 2.2$ (Ludwig et al., 2002; Lee et al., 2015). At high altitudes, n becomes small and hence $D_{\rm micro}$ large, and $\langle v_z \rangle$ becomes small, hence $D_{\rm mix}$ small. We take both processes into account by summing up

$$D \;=\; D_{\rm mix} + D_{\rm micro} \;. \tag{8}$$

2 Solution method

2.1 Vertical grid and discretisation of derivatives

We introduce an ascending vertical grid z_i $(i = 1, ..., I)$. The first and second derivatives of any quantity $f(z_i) = f_i$ at grid point z_i are approximated as

$$\frac{df_i}{dz} \;=\; d_i^{l,1} f_{i-1} + d_i^{m,1} f_i + d_i^{r,1} f_{i+1} \tag{9}$$

$$\frac{d^2 f_i}{dz^2} \;=\; d_i^{l,2} f_{i-1} + d_i^{m,2} f_i + d_i^{r,2} f_{i+1} \;, \tag{10}$$

i.e. as linear combinations of the function values on the neighboring grid points, where e.g. $d_i^{l,1}$ is the coefficient for the first derivative on the point left of the grid point i, $d_i^{m,1}$ the same on the mid point and $d_i^{r,1}$ the same on the point right of grid point i. Similar, for the second derivative, the coefficients are $d_i^{l,2}$, $d_i^{m,2}$ and $d_i^{r,2}$. Using a second-order polynomial approximation for function

$f(z)$ the coefficients are given by

$$d_i^{l,1} = -\frac{h_i^r}{(h_i^r + h_i^l)\, h_i^l} \tag{11}$$

$$d_i^{m,1} = +\frac{h_i^r - h_i^l}{h_i^l h_i^r} \tag{12}$$

$$d_i^{r,1} = +\frac{h_i^l}{(h^r(i) + h_i^l)\, h_i^r} \tag{13}$$

$$d_i^{l,2} = +\frac{2}{(h_i^r + h_i^l)\, h_i^l} \tag{14}$$

$$d_i^{m,2} = -\frac{2}{h_i^r h_i^l} \tag{15}$$

$$d_i^{r,2} = +\frac{2}{(h_i^r + h_i^l)\, h_i^r} \tag{16}$$

where $h_i^l = z_i - z_{i-1}$ and $h_i^r = z_{i+1} - z_i$ are the l.h.s. and the r.h.s. grid point distances. Note that for the special case of an equidistant grid, we have $h = h_i^l = h_i^r$ and hence

$$\frac{df_i}{dz} = \frac{f_{i+1} - f_{i-1}}{2h} \tag{17}$$

$$\frac{d^2 f_i}{dz^2} = \frac{f_{i+1} - 2f_i + f_{i-1}}{h^2} \tag{18}$$

The above equations are valid for grid points $i = 2, \ldots, I-1$. For the first derivative at the boundaries we write

$$\frac{df_1}{dz} = d_1^{l,1} f_1 + d_1^{m,1} f_2 + d_1^{r,1} f_3 \tag{19}$$

$$\frac{df_1}{dz} = d_I^{l,1} f_{I-2} + d_I^{m,1} f_{I-1} + d_I^{r,1} f_I \tag{20}$$

which is also second-order accuracy by using the information on the 3 leftmost or 3 rightmost grid points, respectively. The coefficients are given by

$$d_1^{l,1} = -\frac{h_2 + h_3}{h_2 h_3} \tag{21}$$

$$d_1^{m,1} = \frac{h_3}{h_2(h_3 - h_2)} \tag{22}$$

$$d_1^{r,1} = -\frac{h_2}{h_3(h_3 - h_2)} \tag{23}$$

$$d_I^{r,1} = \frac{h_{I-1} + h_{I-2}}{h_{I-1} h_{I-2}} \tag{24}$$

$$d_I^{m,1} = -\frac{h_{I-2}}{h_{I-1}(h_{I-2} - h_{I-1})} \tag{25}$$

$$d_I^{l,1} = \frac{h_{I-1}}{h_{I-2}(h_{I-2} - h_{I-1})} \tag{26}$$

where $h_2 = z_2 - z_1$, $h_3 = z_3 - z_1$, $h_{I-1} = z_I - z_{I-1}$ and $h_{I-2} = z_I - z_{I-2}$.

2.2 Spatial derivatives

The diffusion term at grid point z_i ($i = 2, \ldots, I-1$) is numerically resolved as

$$\begin{aligned}
\frac{d}{dz}\left(n_{\langle \mathrm{H}\rangle,\mathrm{i}} D_i \frac{d\epsilon_{k,i}}{dz}\right) &= \frac{d(n_{\langle \mathrm{H}\rangle,\mathrm{i}} D_i)}{dz}\,\frac{d\epsilon_{k,i}}{dz} \;+\; n_{\langle \mathrm{H}\rangle,\mathrm{i}} D_i \frac{d^2\epsilon_{k,i}}{dz^2} \\
&= \left(d_i^{l,1} n_{\langle \mathrm{H}\rangle,\mathrm{i}-1} D_{i-1} + d_i^{m,1} n_{\langle \mathrm{H}\rangle,\mathrm{i}} D_i + d_i^{r,1} n_{\langle \mathrm{H}\rangle,\mathrm{i}+1} D_{i+1}\right) \\
&\quad \cdot \left(d_i^{l,1}\epsilon_{k,i-1} + d_i^{m,1}\epsilon_{k,i} + d_i^{r,1}\epsilon_{k,i+1}\right) \\
&+ \; n_{\langle \mathrm{H}\rangle,\mathrm{i}} D_i \left(d_i^{l,2}\epsilon_{k,i-1} + d_i^{m,2}\epsilon_{k,i} + d_i^{r,2}\epsilon_{k,i+1}\right) \qquad (27)
\end{aligned}$$

and the diffusive fluxes accross the lower and upper boundaries are

$$j_{k,1} = -n_{\langle \mathrm{H}\rangle,1} D_1 \frac{d\epsilon_{k,1}}{dz} = -D_1 n_{\langle \mathrm{H}\rangle,1}\left(d_1^{l,1}\epsilon_{k,1} + d_1^{m,1}\epsilon_{k,2} + d_1^{r,1}\epsilon_{k,3}\right) \qquad (28)$$

$$j_{k,I} = -n_{\langle \mathrm{H}\rangle,\mathrm{I}} D_I \frac{d\epsilon_{k,I}}{dz} = -D_I n_{\langle \mathrm{H}\rangle,\mathrm{I}}\left(d_I^{l,1}\epsilon_{k,I-2} + d_I^{m,1}\epsilon_{k,I-1} + d_I^{r,1}\epsilon_{k,I}\right)\ . \qquad (29)$$

2.3 Boundary conditions

As boundary conditions, we have three options. For example, considering the lower boundary:

1. fixed concentration: $\epsilon_{k,1}$ is a given constant
2. fixed flux: $j_{k,1}$ is a given constant
3. fixed outflow rate: The flux through a boundary is assumed to be proportional to the concentration of species k at the boundary, e.g.

$$j_{k,1} = \beta_k\, n_{\langle \mathrm{H}\rangle,1}\, \epsilon_{k,1}\, v_{k,\mathrm{th}} \qquad [\mathrm{cm}^{-2}\mathrm{s}^{-1}] \qquad (30)$$

   where the β_k is a given probability (fixed value) and $v_{k,\mathrm{th}}$ is the speed at which the particles of kind k move through the boundary (also fixed value).

2.4 Explicit time-integration

A straightforward way to integrate Eq. (4), using a timestep Δt, is the following explicit scheme

$$f_i^n = f_i^{n-1} + \Delta t \frac{df_i^{n-1}}{dt} \qquad (31)$$

where f_i^n is some quantity on grid point i at time t^n and f_i^{n-1} is the quantity on grid point i at time t^{n-1} with $t^n = t^{n-1} + \Delta t$. In consideration of Eq. (4), this leads to

$$\epsilon_{k,i}^n = \epsilon_{k,i}^{n-1} + \Delta t \left(\sum_{j=1}^{I} A_{ij}\epsilon_{k,j}^{n-1} + \frac{S_i^{n-1}}{n_{\langle \mathrm{H}\rangle,\mathrm{i}}}\right)\ , \qquad (32)$$

where $\mathbf{A}$ is a tri-diagonal matrix, the elements A_{ij} of which are given by Eq. (27). Equation (32) applies to the grid points $i = 2, \ldots, I-1$, but not to the boundaries. On the boundary points, the following equations are applied depending on the choice of boundary conditions, here for example the lower boundary

1. fixed concentration: $\epsilon^n_{k,1} = \epsilon^{n-1}_{k,1}$

2. fixed flux: $\epsilon^n_{k,1} = \frac{1}{d_1^{l,1}} \left(-\frac{j_{k,1}}{D_1 n_{\langle \mathrm{H} \rangle,1}} - d_1^{m,1} \epsilon^n_{k,2} - d_1^{r,1} \epsilon^n_{k,3} \right)$

3. fixed outflow rate: From $j_{k,1} = -D_1 n_{\langle \mathrm{H} \rangle,1} \left(d_1^{l,1} \epsilon^n_{k,1} + d_1^{m,1} \epsilon^n_{k,2} + d_1^{r,1} \epsilon^n_{k,3} \right) = \beta_k \, n_{\langle \mathrm{H} \rangle,1} \, \epsilon_{k,1} \, v_{k,\mathrm{th}}$ we find
$$\epsilon^n_{k,1} = \frac{-d_1^{m,1} \epsilon^n_{k,2} - d_1^{r,1} \epsilon^n_{k,3}}{d_1^{l,1} + \frac{\beta_k \, v_{k,\mathrm{th}}}{D_1}} \quad .$$

To guanantee numerical stability, the explicit timestep must be limited by $\alpha \leq 0.5$ according to

$$\Delta t \;=\; \alpha \min_{i=2,\,\ldots\,,I} \frac{(z_i - z_{i-1})^2}{\frac{1}{2}(D_i + D_{i-1})} \; . \tag{33}$$

2.5 Implicit integration

To avoid the timestep limitation, and to guarantee numerical stability for much larger timesteps, an implicit integration scheme will be used

$$f_i^n \;=\; f_i^{n-1} + \Delta t \frac{df_i^n}{dt} \tag{34}$$

which is a system of linear equations for the unknowns f_i^n. In consideration of Eq. (4), we have

$$\epsilon^n_{k,i} \;=\; \epsilon^{n-1}_{k,i} + \Delta t \left(\sum_{j=1}^{I} A_{ij} \epsilon^n_{k,j} + \frac{S_i^{n-1}}{n_{\langle \mathrm{H} \rangle,\mathrm{i}}} \right) \tag{35}$$

We re-write this equation more generally, including the boundary conditions as, by means of another unit-free matrix as

$$\mathbf{B} \, \vec{\epsilon}^{\,n}_k \;=\; \vec{R}_k \; , \tag{36}$$

where we have

$$B_{ij} = (\mathbb{1} - \Delta t \mathbf{A})_{ij} \quad \text{and} \quad R_{k,i} = \epsilon^{n-1}_{k,i} + \Delta t \frac{S_i^{n-1}}{n_{\langle \mathrm{H} \rangle,\mathrm{i}}} \qquad \text{for } i = 2,\, \ldots\,, I-1 \tag{37}$$

and, depending on boundary conditions, for example at the lower boundary

1. fixed concentration: $B_{11} = 1$ and $R_{k,1} = \epsilon^{n-1}_{k,1}$

2. fixed flux: $B_{11} = 1$, $B_{12} = d_1^{m,1}/d_1^{l,1}$, $B_{13} = d_1^{m,1}/d_1^{l,1}$, and $R_{k,1} = -j_{k,1}/\left(n_{\langle \mathrm{H} \rangle,1} D_1 d_1^{l,1}\right)$

3. fixed outflow rate: $B_{11} = 1 + \beta_k \, v_{k,\mathrm{th}}/\left(D_1 d_1^{l,1}\right)$, $B_{12} = d_1^{m,1}/d_1^{l,1}$, $B_{13} = d_1^{m,1}/d_1^{l,1}$ and $R_{k,1} = 0$.

We can now perform an implicit timestep according to Eq. (36) as

$$\vec{\epsilon}^{\,n}_k \;=\; \mathbf{B}^{-1} \, \vec{R}_k \tag{38}$$

where $\mathbf{B}^{-1}$ is the inverse of the matrix $\mathbf{B}$. As long as the the spatial grid points z_i, the densities $n_{\langle \mathrm{H} \rangle,\mathrm{i}}$ and diffusion constants D_i, the constants involved in the boundary conditions (e.g. $j_{k,1}$ or β_k), and the timestep Δt does not change, we need to perform the matrix inversion only once.

Successive time steps are then performed by simply incrementing n, re-computing the vector $\vec{R}_k$, and applying again Eq. (38). $\mathbf{B}^{-1}$ is also usually the same for all elements k to be diffused.

This favourable property of $\mathbf{B}$ makes the computation of implicit timesteps actually very fast. We note, however, that $\mathbf{B}^{-1}$, in general, is a full $I \times I$ matrix where all entries are positive $(\mathbf{B}^{-1})_{ij} > 0$. This leads to a very stable numerical behaviour for arbitrary time steps. In contrast, the matrix $\mathbf{A}$ has positive entries along the main diagonal, but negative entries along both semi-diagonals, which leads to numerical instabilities when the time step is too large.

3 Test results

Figures 1 to 4 show a few test problems on domain $z = 0 \ldots 1$, with constant $n_{\langle \mathrm{H} \rangle} = 1$ and $D = 1$. The third and forth test problem have overplotted analytic solutions. All tests use an equidistant z-grid with 101 points, use the implicit solver, and can be computed within less than 1 CPU-sec.

References

Bringuier, E. (2013). The Maxwell-Stefan description of binary diffusion. *European Journal of Physics* **34**(5), 1103.

Lee, G., Helling, C., Dobbs-Dixon, I., Juncher, D. (2015, August). Modelling the local and global cloud formation on HD 189733b. *A&A* **580**, A12.

Ludwig, H.-G., Allard, F., Hauschildt, P. H. (2002, November). Numerical simulations of surface convection in a late M-dwarf. *A&A* **395**, 99–115.

Woitke, P., Helling, C. (2003, February). Dust in brown dwarfs. II. The coupled problem of dust formation and sedimentation. *A&A* **399**, 297–313.

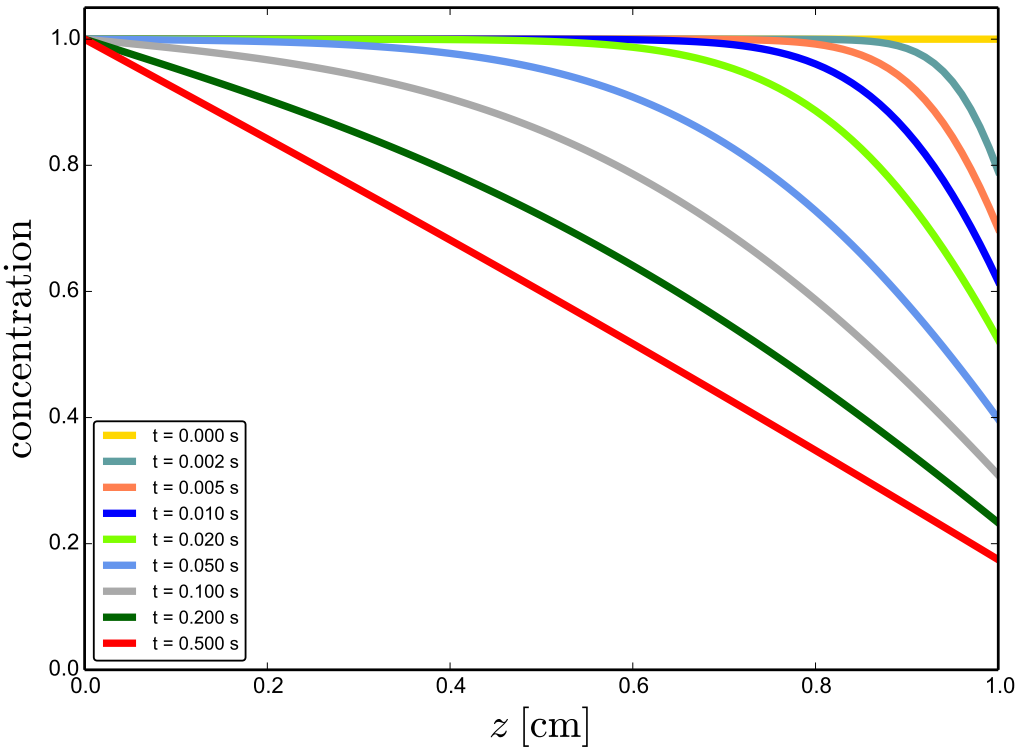

Figure 1: Test problem with fixed concentration on the left ($\epsilon = 1$), and fixed outflow rate ($\beta = 5$) on the right. Near t=0.5 s, the concentration has reached a steady state where elements are constantly transported rightways.

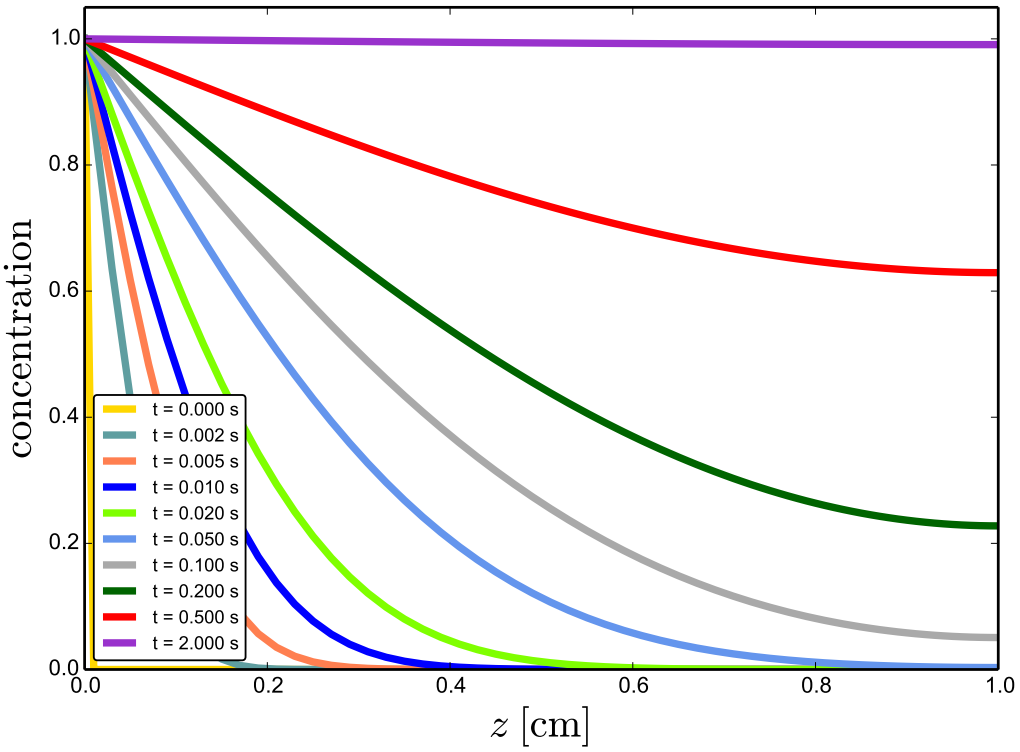

Figure 2: Test problem with fixed concentration on the left ($\epsilon = 1$), and fixed flux ($j = 0$) on the right. The time-independent solution $\epsilon = 1$ is reached at about 2 s.

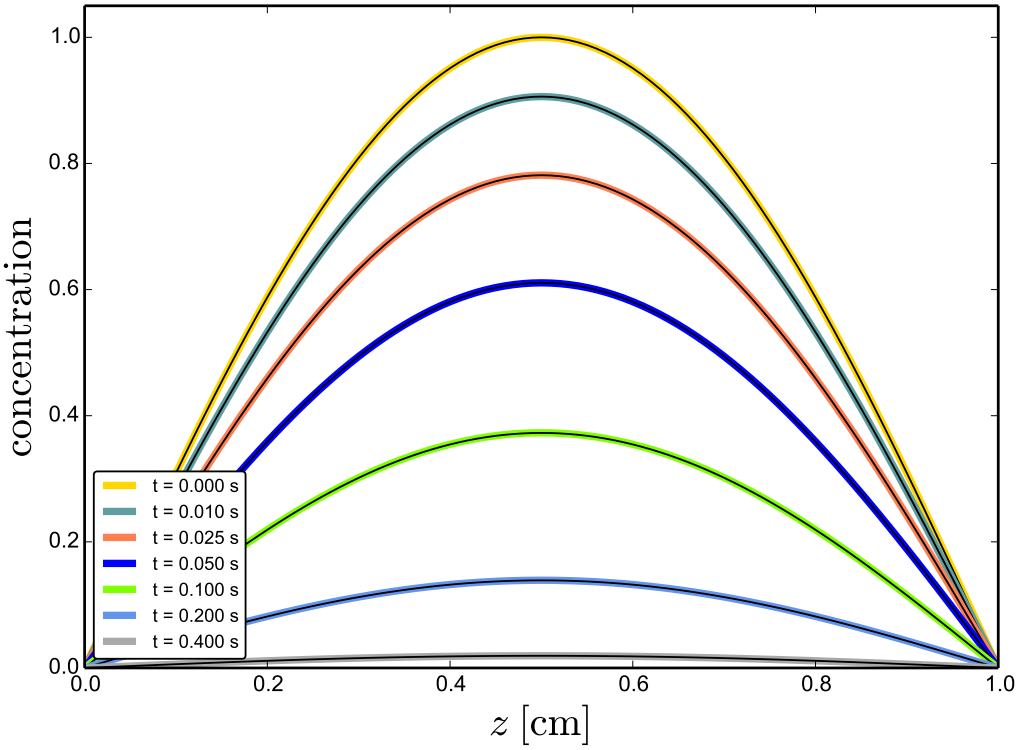

Figure 3: Test problem with fixed concentrations on the left and right sides ($\epsilon = 0$). The thin black lines overplot the analytic solution $\epsilon(z,t) = \exp(-\omega t)\sin(kz)$ with $k = \pi$ and $\omega = Dk^2$.

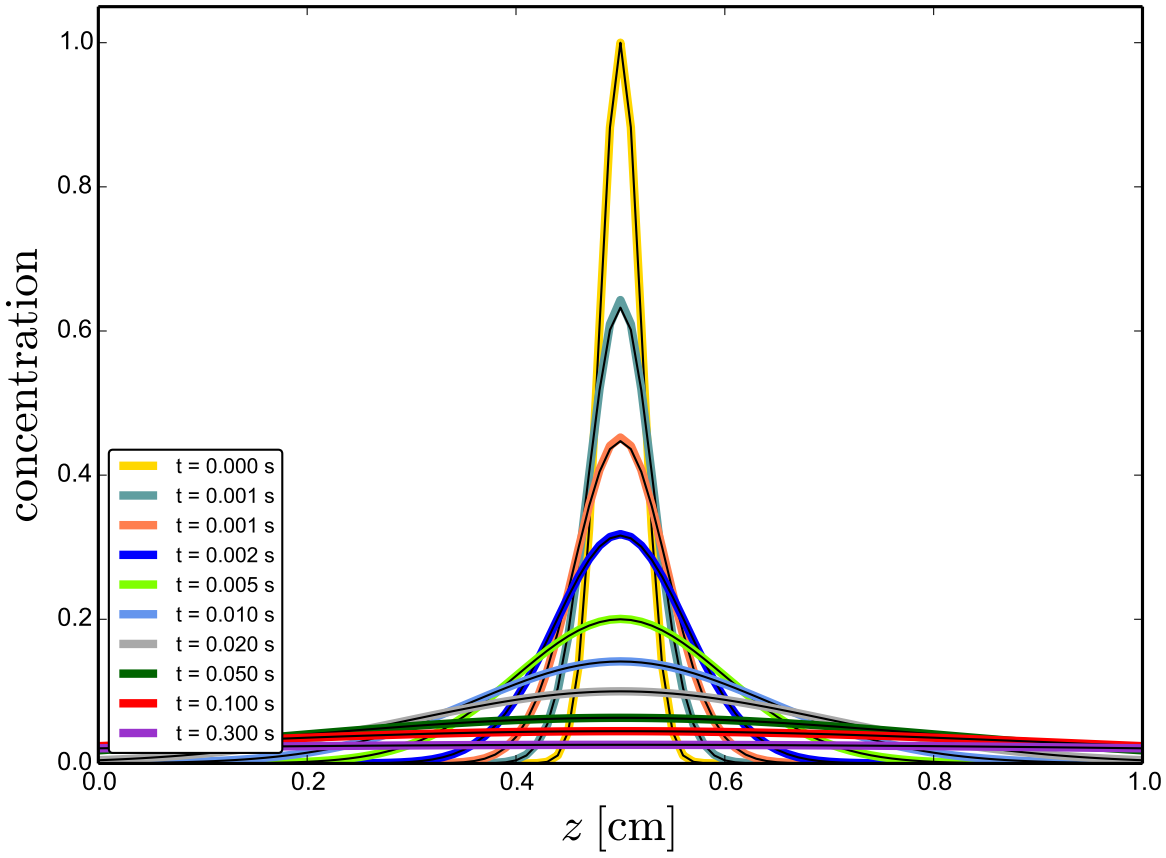

Figure 4: Diffusive evolution of an initial δ-peak with analytic solution overplotted. The analytic solution is $\epsilon(z,t) = A(t)\exp\big(-(z-0.5)^2/w^2(t)\big)$ with $A(t) = \sqrt{t_0/t}$ and $w(t) = 2\sqrt{Dt}$.